This is a postprint version of the following published document:

Cuadrado, M., Artero-Guerrero, J. A., Pernas-Sánchez, J., & Varas, D. (2019). Model updating of uncertain parameters of carbon/epoxy composite plates from experimental modal data. Journal of Sound and Vibration, 455, 380-401

doi:https://doi.org/10.1016/j.jsv.2019.05.007

© Elsevier, 2019

This work is licensed under a Creative Commons Attribution-NonCommercialNoDerivatives 4.0 International License.

Model updating of uncertain parameters of carbon/epoxy composite plates from experimental modal data

M. Cuadrado[a,b,*], J.A. Artero-Guerrero[a], J. Pernas-Sánchez[a], D. Varas[a]

[a] *Department of Continuum Mechanics and Structural Analysis. University Carlos III of Madrid. Avda. de la Universidad, 30. 28911 Leganés, Madrid, Spain*
[b] *Fundación Caminos de Hierro, C/ Serrano 160, 28002 Madrid, Spain*

Abstract

This work presents a methodology to obtain physically-sound models of composite structure laminates using a combination of modal analysis, numerical modelling and parameter updating, avoiding the common uncertainties on the constructions of similar numerical models. Moreover this model establishes the baseline (pristine situation) of the dynamic behaviour of the set of composite plates. Therefore it could be applied for condition assessment or quality manufacturing control of existing structures through a non-destructive Structural Health Monitoring (SHM), and hence it could help to detect degradation or defects of the composite components. The driven data of the methodology were the modal frequencies and shapes of composite plates. To obtain these values an extensive experimental campaign of modal analysis has been performed on a set of carbon/epoxy laminates. A multiple input single output technique has been applied, using a roving hammer exciting the plates at evenly distributed Degrees of Freedom (DoF),

*corresponding author: M. Cuadrado (sanguino@ing.uc3m.es)

and a mono-axial accelerometer attached to a single DoF reference point. The use of a high dense grid of points has allowed to identify a number of natural frequencies greater than usual in similar works, as well as improving the smoothness of the mode shape. Modal characteristics numerically obtained from a Finite Element Method (FEM) model based on manufacturer reference data were compared with experimental results. This baseline model was updated through a gradient based optimization algorithm. Before the process of model updating, a sensitivity analysis has been performed to identify the driven uncertain parameters using a Montecarlo approach. This technique reduces the number of parameters to be optimized to a small set increasing the efficiency of the methodology. As a result of the whole process, a physically more accurate model is obtained on which discrepancies with the corresponding experimentally measured modal parameters are drastically reduced. Analysis of the consistency of the adjusted numerical parameters has been done with alternative experimental tests (Quasi Static Loading (QSL) and Ultrasonic inspection).

Keywords: Model updating; Experimental modal data; Uncertain mechanical properties; Carbon/epoxy composite

1. Introduction

Composite laminates are broadly used in advanced structural engineering, particularly in weight sensitive applications. This spread is pushing the industry to develop new manufacturing low-cost techniques which implies variability in the final parts, and hence new efficient techniques of early detection of defects and quality control are needed. Moreover, for Structural

Health Monitoring (SHM), as these materials are vulnerable to impact damage, the topic of efficient techniques to detect damage at an early stage, specially in the case of Barely Visible Damage (BVD), has become an issue of great concern [1].

Among many different methods, the evaluation of changes in modal parameters of the structure between the pristine and defective states, has been intensively studied by many researchers over the last three decades. These changes can be used as a good indicator to detect, localize and quantify the defects [1–3], and is one of the most widely adopted methods. The basic idea is that the presence of defects in structures involves variations of its dynamic response, that can be explained because of the consequential changes in the dynamic properties of the structure. In the case of civil engineering, some of these strategies are based on the estimation of modal parameters from vibration data obtained under operational conditions and mainly applied to beam-like structures or trusses [4–6]. Recently the attention has been also focused on two-dimensional structures such as plates or shells [7].

Many of these researchers have applied these methods to damage assessment of composite plate structures, using different vibration-based methods [1, 7–12]. Even though some of these methods are based solely in the analysis of the experimental data to identify damage, most of them use numerical models (based on Finite Element Models (FEM)) for the reference pristine situation. Although a priori FEM, based on theoretical properties of the structure, provides useful information, such a model cannot predict the modal parameters with a high level of accuracy, due to some uncertainties about its mechanical properties. In the case of composite materials, tests performed on two specimens of the same structural model can display very different dynamic behaviour due to large uncertainties associated with composite material properties or pre-existing imperfections [13].

Model updating techniques have been widely applied to adjust theoretical structural models using modal data obtained experimentally in civil and industrial engineering during the last three decades [14–17], but also more recently for composite plates [18–22]. Model updating procedure can be treated as a problem of optimization, in which the weighted differences between experimental and theoretical values of some of the modal characteristics of the structure are computed to obtain the objective function.

The present work consists on the development of a reference numerical model, updated through modal parameters experimentally obtained, that establishes the baseline (pristine situation) of the dynamic behaviour of a set of carbon/epoxy composite plates. The methodology starts with the development of a numerical model (FEM) of the plates built in ANSYS by using solid elements [23]. Then, a model updating using experimental modal parameters is performed. To obtain the modal characteristics of the plates, a modal testing was performed using a roving hammer exciting the plates at evenly distributed positions, and a mono-axial accelerometer attached to a single Degree of Freedom (DoF) reference point. The vibration data are treated by Modal Analysis of Civil Engineering Constructions (MACEC) program

[24]. After modal identifications, considerable discrepancies between the numerically calculated and the corresponding experimentally measured modal characteristics of the plates have been identified, mainly due to uncertainties on the manufacturer provided values of physical parameter of the model. Thus, the updating parameters are the global characteristics of the plate for which a certain uncertainty exists due to inherent manufacturing process of composite structures (hand or automatic lay-up, curing process...). As a result of the whole process, a physically more accurate model is obtained on which discrepancies with the corresponding experimentally measured modal parameters are drastically reduced. The analysis of the consistency of the adjusted parameters has been done with additional tests.

Apart from the direct interest of having determined more realistic mechanical characteristics of the plates, this reference model can be used for both, the prediction of the dynamic behaviour and the detection and localization of defects induced in structures composed by this kind of plates. Some of the contributions of this study are the high accuracy reached in the experimental modal analysis, with up to 22 modes identified, number much higher than usually reached in this kind of works [18–22], and the automatization of mode pairing needed for model updating algorithms considering such a great number of modes during optimization process. Additionally, it is also innovative the use of extensive Monte Carlo Simulations (MCS) to perform sensitivity analysis of the potentially updated parameters. As a result it has been obtained an efficient model updating methodology which is able to produce an accurate physically-sound numerical model. Finally the efficiency of the methodology has been proved through benchmarking test.

The description of the specimens of carbon/epoxy composite plates used for the work and a summary of experimental modal test procedures as well as the results of experimental modal analysis are reported in Section 2. The preliminary FEM based on the provided manufacturer mechanical properties of the plates is addressed in Section 3. Model updating is described on section 4, including mode pairing and a sensibility analysis by which the material properties with higher influence on modal parameters are identified. Finally, several variants of objective functions are minimized using ANSYS algorithms to solve the optimization problem [23]. In section 5 the experimental validation of some of the updated properties of the plates is made. Section 6 presents the results of the benchmarking test performed on a second set of composite plates. Conclusions are included in the last section.

2. Tests procedure

The experimental programme involved mainly the modal testing of all the specimens. In addition a ultrasonic inspection was carried out to determine the real value thickness of the plates and to assure the absence of damage (delamination). Finally, quasistatic loading test was performed to measure the real stiffness of the laminates. Two sets of composite plates have been studied in the present work: the first, drive set composed by four specimens of 21 plies laminate each, has been used to develop the methodology; while, the second, benchmarking set composed by six specimens of 32 plies laminate each, has been used to prove its efficiency.

Property	**Value**
Young modulus in fibre direction (E_1)	139 GPa
Young modulus in transverse direction ($E_2 = E_3$)	9 GPa
Shear modulus($G_{12} = G_{13}$)	5 GPa
Shear modulus(G_{23})	4.5 GPa
Poisson's ratio ($\nu_{12} = \nu_{13} = \nu_{23}$)	0.308
Density (ρ)	1580 kg/m^3

Table 1: Nominal properties of the plies

2.1. Specimens description

Composite plate specimens composed of AS4 carbon fibres embedded in an 8552 resin epoxy matrix manufactured by HEXCEL have been used. The quasi-isotropic laminated plates were composed of 21 and 32 unidirectional prepeg laminae with a theoretical thickness of 0.19 mm. Driven set has a symmetric stacking sequence $(45/-45/90/0/90/-45/45/90/0/90/0)_{s'}$ while benchmarking set is $(45/-45/90/0/90/-45/45/90/0/90/45/-45/90/90/-45/45)_s$, resulting in a nominal thickness of the plates of approximately 4 and 6 mm, with a theoretical uniform cross-section over the entire surface. The plates have been cut to obtain $300 \times 300\ mm^2$ specimens (Fig. 1). Curing was performed following a standard autoclave procedure by the "*Instituto Nacional de Tecnicas Aeroespaciales (INTA)*". Nominal properties of the laminae provided by the manufacturer are shown on Table 1 (where 1 axis is coincident with the fibre direction).

2.2. Experimental modal testing

To obtain the modal characteristics of the four plates, a modal testing was performed under free boundary conditions (by suspending the plates, alternatively, horizontally and vertically using rubber bands and nylon threads respectively). The excitation of the plates has been done using a roving hammer at 120 DoFs evenly distributed in both directions (every 25 mm). A mono-axial accelerometer was attached to a single DoF reference point [point 1 on the corner of the plate as seen in Fig. 1].

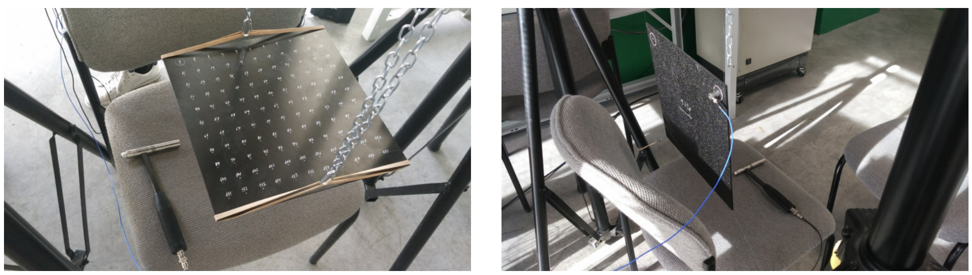

(a) horizontal position (b) vertical position

Figure 1: Specimen and test set-up simulating free boundary conditions

Two channels of the data acquisition system have been used, one for the exciter hammer, and the other for the accelerometer. The characteristics of accelerometer and hammer are the following:

- Accelerometer: PCB Piezotronics model 352C33; sensitivity 10.19 mV/m/s^2; Measuring range 0.5-10000 Hz

- Hammer: PCB Piezotronics model 086C03; sensitivity 2.25 mV/N; measurement range $\pm$ 2224 N pk; mass 0.16 kg.

Three seconds of the signals are recorded at a sampling frequency of 10 kHz. Fig. 2 shows examples of the recorded signals.

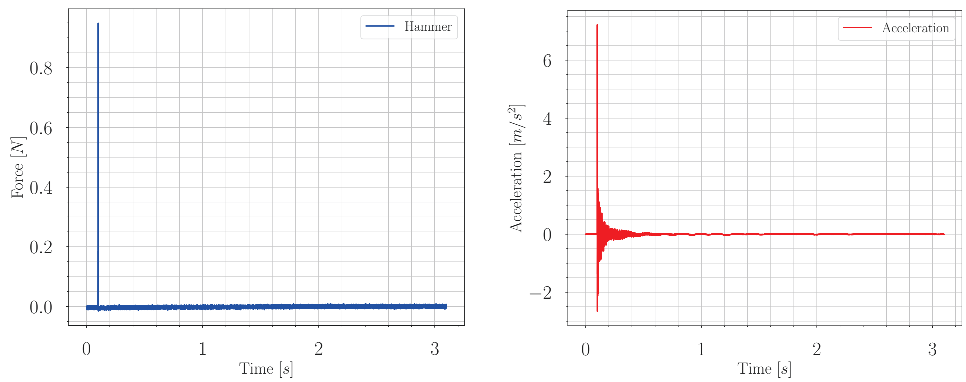

(a) Hammer (b) Accelerometer

Figure 2: Example of signals recorded

The determination of the FRFs is carried out using the Tri-spectrum averaging method, which involves the determination of three spectra, the auto-power spectrum (APS) of each of the signals (hammer and accelerometer) and the cross-power spectrum between both signals (XPS) [25]. Even though there is noise in both the accelerometer signal (output) and the hammer (input), it has been seen that better results were obtained by applying the H_2 method (instead of recommended HV method). The H_2 method calculates the FRF as:

$$H_2 = \frac{Output\ APS}{XPS} \tag{1}$$

In the FRF (magnitude) calculated for impact at point 2 is shown in Fig. 3 as an example. Once calculated the FRF corresponding to the 120 points of impact (see Fig. 3), its average is calculated.

As can be seen in Fig. 4, abovementioned average reduces the noise of

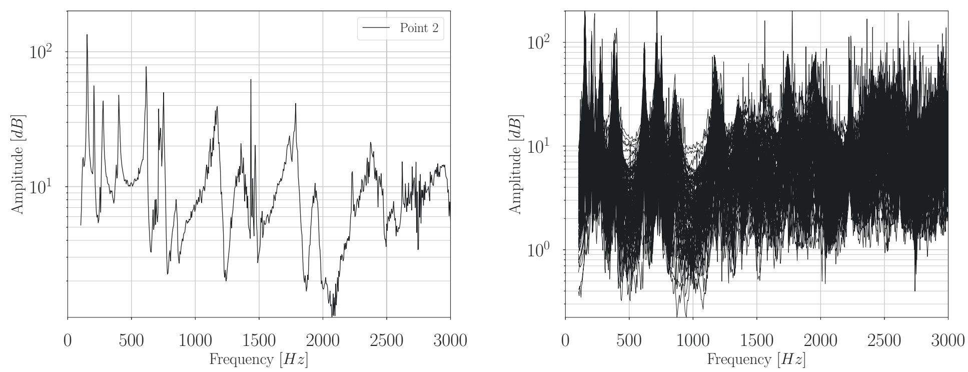

(a) Point 2 (b) All the points

Figure 3: Computed FRFs

the functions and would allow to identify, by pick-picking, the position of the plate's natural frequencies, in the maximums of the magnitude. As the picks are almost identical for the four plates, the pick-picking has been done for the average FRF of the four plates, as can be seen in Fig. 4. It must be pointed out that also very similar results have been obtained with the two ways of simulating free boundary conditions.

However, a parametric identification usually obtains more precise results, and that is why identification has been carried out using the poly-reference least squares complex frequency domain method (pLSCF method) [24]. Given that most of the modes have been identified in the four plates with very stable values of the frequency, the data have been processed as corresponding to four different setups of the same test. the average values of frequencies and modal forms were identified improving the accuracy of the test. These values of the 22 identified frequencies are shown in Table 2, in which the type (a, b) indicates the number of nodal lines parallel to

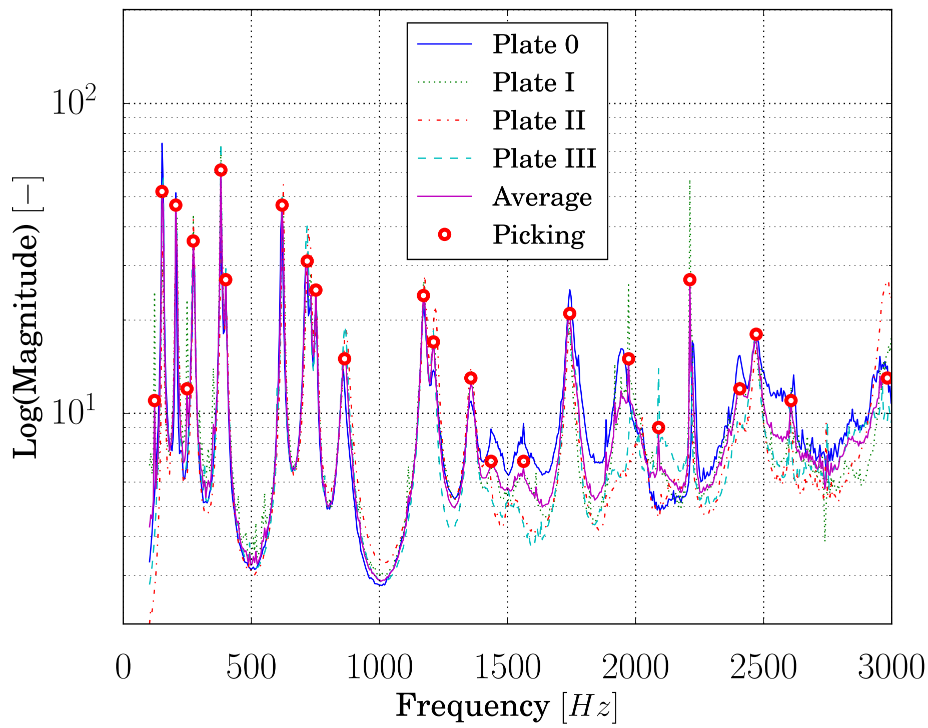

Figure 4: Averaged FRFs for the four plates tested

the crosswise and lengthwise direction, respectively, of the transverse corresponding mode shapes as shown in Fig. 11. Given that both, excitation and measurements, are perpendicular to the plate surface, only out of laminate plate modes have been identified.

MAC (modal assurance criterion) values have also been calculated between the identified mode shapes. The MAC values provide a scalar correlation criterion that indicates the degree of coherence or correlation between two modal vectors [26], expressed as:

$$MAC\left(\phi_i, \phi_j\right) = \frac{\left|\phi_i^T \phi_j\right|^2}{\phi_i^T \phi_i \phi_j^T \phi_j} \tag{2}$$

Nº	**Type**	**f (Hz)**	**Nº**	**Type**	**f (Hz)**
1	(1 1)	154	12	(1 4)	1359
2	(0 2)	207	13	(4 0)	1433
3	(2 0)	273	14	(4 1)	1545
4	(1 2)	382	15	(3 3)	1740
5	(2 1)	401	16	(2 4)	1777
6	(0 3)	622	17	(4 2)	1928
7	(3 0)	717	18	(0 5)	1987
8	(1 3)	753	19	(1 5)	2092
9	(3 1)	864	20	(3 4)	2405
10	(2 3)	1174	21	(4 3)	2469
11	(3 2)	1215	22	(0 6)	2973

Table 2: Natural frequencies obtained with pLSCF averaging results of the four plates

Where ϕ_i and ϕ_j are modal vectors, which contain the n values of the modal deformation of the vibration modes i and j respectively, experimentally estimated at the n measurement points (120 in the present case). MAC values are in the range between 0 and 1, where the minimum value indicates zero coherence and the maximum value a perfect coherence between both mode shapes. Fig. 5 shows the MAC values calculated between experimentally identified modes. Obviously, the values of the diagonal are all 1, since they indicate the correlation of each mode with itself. On the other hand, the almost null values outside the diagonal indicate that the identified modes are linearly independent.

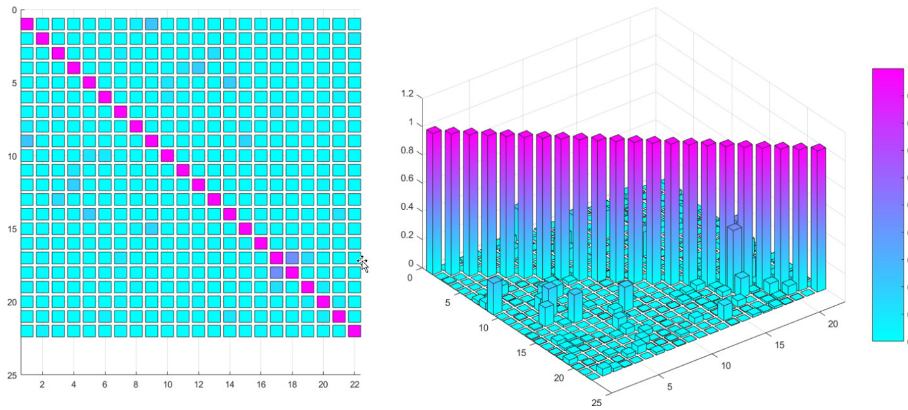

Figure 5: The MAC values between the 22 modes experimentally identified

3. Preliminary FEM model

The results of the experimental estimation are compared with the results of the analysis on a FEM model of the plates, for which ANSYS software has been used.

One of the main goal is to obtain a physically-sound model that could eventually be used to simulate the presence of intra and interlaminar damage. Therefore it is advisable to have at least an element in the thickness of each ply, being possible to model the interlaminar failure disconnecting the nodes between elements. Hence, the type of element that best fits the objectives of the model is the hexahedron (SOLID45 in Ansys notation).

Additionally, a mass element has been included to idealize the presence of the accelerometer used in the experimental determination of the modal characteristics (Fig. 6). This mass, although small (it is 5.8 g.), cannot be considered as negligible and must be included in the model to obtain a greater approximation between numerical and experimental results, especially for some of the modal forms. As well as the experimental setup, free boundary condition were considered for the plates.

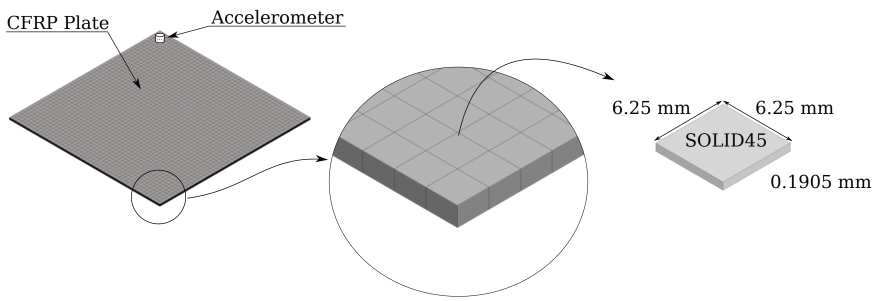

Figure 6: FEM of the plates: position of the mass element that idealizes the accelerometer and mesh

The smaller dimension of the element will coincide with the thickness of each of the 21 sheets of the plate, that is, 0.1905 mm. Regarding the larger dimension, a sensitivity analysis was carried out with values of the element size between 25 and 2.5 mm. Fig.7 shows the percentage of variation of natural frequencies obtained by modal analysis on each element size, with respect to the previous one. As can be observed up to an element size of 6.25 mm, the percentage of variation is appreciable, but by reducing the size of the element to 2.5 mm the differences are lower than 1% in most of the modes, with a maximum of 2%. Therefore, it has been considered that the size of 6.25 mm is adequate, combining a sufficient precision without significantly increasing the computational cost. The result is the fine mesh that can be seen in Fig. 6, including 48384 elements and 52822 nodes.

With this model, the first 34 natural frequencies represented in Table 3

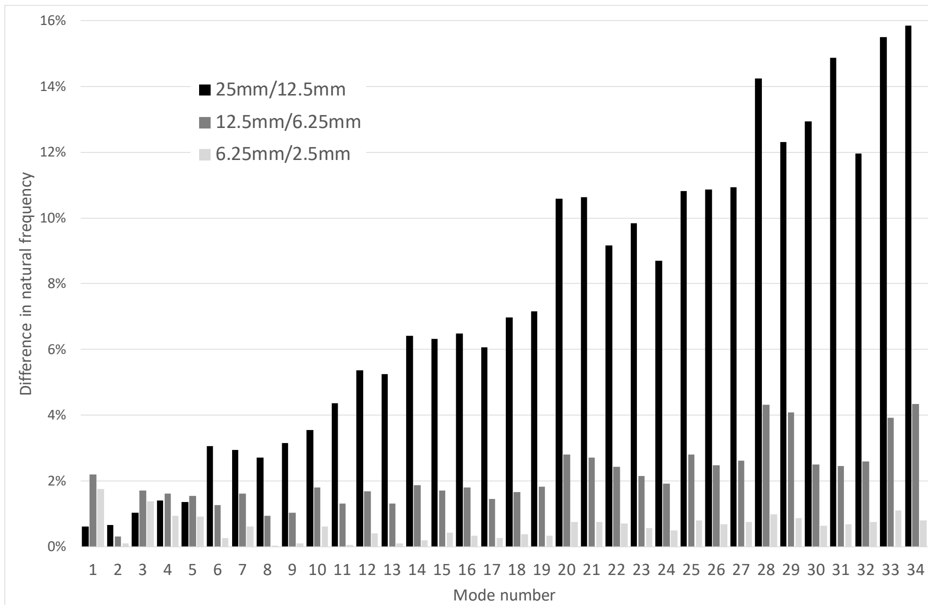

Figure 7: Sensitivity analysis of natural frequencies obtained from the FEM to element size

are obtained. These values were compared with experimental ones in next sections.

4. Model updating

Model updating is the correction process of some theoretical parameters of the numerical models based on experimental data, in this case the identified experimental modal parameters. As above-mentioned, this process will be necessary because the numerical models of the plates will deviate from their real behaviour, due to the variations of the real values of some of the parameters with respect to their theoretical values, such as geometric variations, properties of the materials and the possible appearance of defects such as delamination.

Nº	Type	f (Hz)	Nº	Type	f (Hz)	Nº	Type	f (Hz)
1	(1 1)	171	13	(3 2)	1333	25	(5 1)	2711
2	(0 2)	222	14	(1 4)	1494	26	(2 5)	2818
3	(2 0)	302	15	(4 0)	1569	27	(5 2)	3096
4	(1 2)	418	16	(4 1)	1696	28	(0 6)	3239
5	(2 1)	442	17	(3 3)	1901	29	(1 6)	3392
6	(0 3)	674	18	(2 4)	1939	30	(4 4)	3457
7	(3 0)	793	19	(4 2)	2123	31	(3 5)	3498
8	(2 2)	802	20	(0 5)	2185	32	(5 3)	3730
9	(1 3)	821	21	(1 5)	2317	33	(6 0)	3789
10	(3 1)	966	22	(5 0)	2559	34	(2 6)	3881
11	(2 3)	1283	23	(3 4)	2630			
12	(0 4)	1314	24	(4 3)	2694			

Table 3: 34 first natural frequencies predicted by FEM

The utility of model updating is twofold; on the one hand, it helps in the precise determination of the structural dynamic response of the tested pieces and, on the other hand, it is a very useful tool to be able to establish the effect of possible defects in the pieces.

First, and based on the experimental results obtained from the pristine plates, this procedure tries to find the numerical parameters (essentially density, thickness of the plies and elastic properties of the composite material) that achieve a better fit with experimental results. The process is divided into three main parts: (i) contrast with experimental results, (ii) sensitivity analysis and (iii) parameter adjustment. The contrast with the experimental results consists essentially in the process of mode pairing that is explained below.

4.1. Mode pairing

Mode pairing is the process by which the vibration modes of the numerical model, that correspond to the modes extracted from the experimental analysis, are identified. This pairing is not immediate because the numbers of the numerical and experimental modes will not match in general. As this pairing must be done several thousand times during the model updating (in the different cycles of the optimization algorithm) it is essential to automate the process.

The most commonly used parameter to perform this task is MAC previously defined in ec 2. In this case, ϕ_i are the n modal vectors that contain the values of the modal deformation of the experimentally estimated vibration modes, while the ϕ_j contain the values calculated with the numerical model. For each experimental mode i the corresponding numerical mode J will be the one with the highest MAC value when compared to it; that is, $MAC_{iJ} = max(MAC_{ij})$. Thus, in each numerical model from which we want to compare the modal parameters with the experimental ones, the MACs of all the extracted modes must be calculated with those obtained experimentally to choose in each case the numerical mode that best matches the experimental one.

Fig. 8 shows the MAC values obtained by comparing the 22 experimental modes obtained for the plates with the first 34 modes calculated with the numerical model. It is generally assumed that values greater than 0.8 indicate an adequate coherence value between experimental and numerical mode. In this sense the identification in this case is, in general, very clear, since there are up to 19 pairings with MAC values higher than 0.8, another with a very close value (0.74) and only two with values lower than 0.70 (0.55 and 0.46), as can be seen even more clearly in Figure 9, in which the frequencies of both, numerical and experimental modes, are specified together with corresponding MAC values. Regarding the differences in frequencies between the paired modes, these are around 9% in all modes, as it is seen in figure 10.

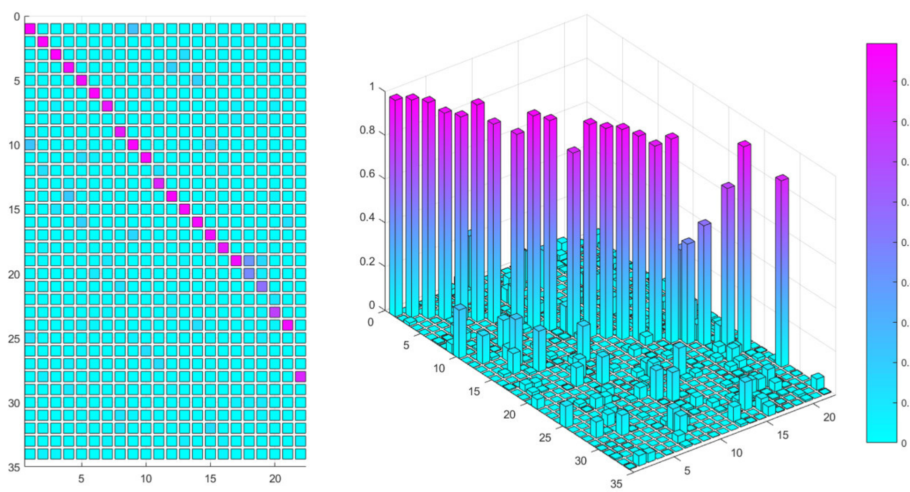

Figure 8: MAC values between 22 experimentally identified and 34 calculated with FEM modes.

Fig. 11 shows the numerical and estimated modal forms for the first 20 modes with a MAC value close to or greater than 0.8.

4.2. Material properties sensitivity analysis

The purpose of the sensitivity analysis is to determine which parameters of the model have the greatest influence on the responses of interest, in this case the vibration mode shapes and eigenfrequencies. Thus, in the next step,

	F exp (Hz)	154	207	273	382	401	622	717	753	864	1174	1215	1359	1433	1545	1740	1777	1928	1987	2092	2405	2469	2973
F fem (Hz)	**mode**	**1**	**2**	**3**	**4**	**5**	**6**	**7**	**8**	**9**	**10**	**11**	**12**	**13**	**14**	**15**	**16**	**17**	**18**	**19**	**20**	**21**	**22**
170.6	**1**	0.99	0.00	0.01	0.00	0.00	0.00	0.03	0.05	0.24	0.00	0.00	0.00	0.00	0.00	0.00	0.00	0.00	0.00	0.04	0.00	0.00	0.00
222.0	**2**	0.00	1.00	0.00	0.00	0.00	0.00	0.00	0.00	0.00	0.00	0.00	0.00	0.01	0.00	0.00	0.04	0.03	0.02	0.00	0.01	0.00	0.05
301.7	**3**	0.01	0.00	0.99	0.00	0.00	0.00	0.06	0.00	0.00	0.00	0.00	0.00	0.14	0.00	0.00	0.02	0.01	0.00	0.00	0.00	0.00	0.02
417.7	**4**	0.00	0.00	0.00	0.95	0.02	0.00	0.00	0.00	0.00	0.01	0.08	0.18	0.00	0.01	0.00	0.00	0.01	0.00	0.00	0.01	0.00	0.00
442.0	**5**	0.00	0.00	0.00	0.01	0.93	0.00	0.00	0.00	0.00	0.06	0.00	0.00	0.00	0.17	0.00	0.00	0.00	0.00	0.00	0.01	0.03	0.00
674.0	**6**	0.00	0.00	0.00	0.00	0.00	0.99	0.00	0.01	0.00	0.09	0.00	0.00	0.00	0.00	0.00	0.00	0.00	0.01	0.00	0.00	0.05	0.00
793.1	**7**	0.00	0.00	0.05	0.00	0.00	0.00	0.91	0.00	0.01	0.00	0.03	0.00	0.01	0.00	0.00	0.00	0.05	0.02	0.00	0.06	0.00	0.00
801.5	8	0.00	0.01	0.03	0.00	0.00	0.00	0.00	0.00	0.00	0.00	0.04	0.00	0.01	0.00	0.00	0.02	0.08	0.04	0.05	0.04	0.00	0.00
821.0	**9**	0.04	0.00	0.00	0.00	0.00	0.00	0.00	0.89	0.01	0.00	0.00	0.00	0.00	0.00	0.03	0.01	0.00	0.00	0.03	0.00	0.00	0.00
966.3	**10**	0.22	0.00	0.01	0.00	0.00	0.00	0.01	0.02	0.98	0.00	0.00	0.00	0.00	0.00	0.15	0.00	0.00	0.00	0.00	0.00	0.00	0.00
1283.5	**11**	0.00	0.00	0.00	0.00	0.13	0.06	0.00	0.00	0.00	0.96	0.00	0.00	0.00	0.01	0.00	0.01	0.00	0.00	0.00	0.00	0.01	0.00
1313.5	12	0.00	0.13	0.01	0.00	0.00	0.00	0.00	0.00	0.00	0.00	0.12	0.01	0.01	0.00	0.00	0.08	0.00	0.01	0.00	0.01	0.00	0.05
1332.8	**13**	0.00	0.00	0.00	0.06	0.00	0.00	0.02	0.00	0.00	0.01	0.84	0.00	0.00	0.00	0.00	0.01	0.00	0.00	0.00	0.02	0.00	0.00
1493.7	**14**	0.00	0.00	0.00	0.21	0.01	0.00	0.00	0.00	0.00	0.00	0.02	0.97	0.00	0.00	0.00	0.00	0.00	0.00	0.00	0.03	0.00	0.00
1568.6	**15**	0.00	0.01	0.10	0.00	0.00	0.00	0.01	0.00	0.00	0.00	0.00	0.00	0.96	0.00	0.00	0.02	0.02	0.00	0.00	0.00	0.00	0.00
1696.4	**16**	0.00	0.00	0.00	0.01	0.19	0.00	0.00	0.00	0.00	0.01	0.00	0.00	0.00	0.96	0.00	0.02	0.01	0.00	0.02	0.01	0.11	0.00
1900.7	**17**	0.01	0.00	0.00	0.00	0.00	0.00	0.00	0.03	0.16	0.00	0.00	0.00	0.00	0.00	0.94	0.00	0.01	0.00	0.01	0.00	0.00	0.00
1939.0	**18**	0.00	0.03	0.02	0.00	0.00	0.00	0.02	0.00	0.00	0.00	0.00	0.00	0.01	0.00	0.04	0.90	0.00	0.00	0.01	0.02	0.00	0.01
2123.3	**19**	0.00	0.02	0.01	0.00	0.00	0.00	0.09	0.00	0.00	0.00	0.00	0.00	0.03	0.00	0.00	0.00	0.93	0.41	0.15	0.00	0.00	0.01
2184.6	**20**	0.00	0.00	0.00	0.00	0.00	0.09	0.00	0.00	0.00	0.02	0.00	0.00	0.00	0.00	0.00	0.01	0.00	0.46	0.07	0.00	0.01	0.01
2316.9	**21**	0.04	0.00	0.00	0.00	0.00	0.00	0.00	0.12	0.00	0.00	0.00	0.00	0.00	0.00	0.02	0.02	0.00	0.00	0.55	0.00	0.00	0.00
2559.2	22	0.00	0.00	0.00	0.00	0.00	0.00	0.00	0.00	0.00	0.00	0.03	0.06	0.01	0.00	0.00	0.00	0.00	0.00	0.01	0.09	0.00	0.00
2630.2	**23**	0.00	0.00	0.00	0.02	0.00	0.00	0.04	0.00	0.00	0.00	0.01	0.07	0.00	0.00	0.00	0.01	0.00	0.01	0.03	0.74	0.00	0.00
2694.3	**24**	0.00	0.00	0.00	0.00	0.05	0.04	0.00	0.00	0.00	0.02	0.00	0.00	0.00	0.13	0.00	0.01	0.00	0.02	0.01	0.04	0.94	0.00
2710.8	25	0.10	0.00	0.00	0.00	0.00	0.00	0.00	0.01	0.05	0.00	0.00	0.00	0.00	0.01	0.02	0.00	0.00	0.00	0.07	0.00	0.01	0.00
2817.9	26	0.00	0.00	0.00	0.00	0.04	0.00	0.00	0.00	0.00	0.14	0.00	0.00	0.00	0.00	0.00	0.00	0.00	0.02	0.03	0.00	0.01	0.00
3096.1	27	0.00	0.00	0.00	0.05	0.00	0.00	0.00	0.00	0.00	0.00	0.13	0.01	0.00	0.00	0.00	0.00	0.00	0.00	0.01	0.00	0.00	0.01
3239.4	**28**	0.00	0.07	0.01	0.00	0.00	0.00	0.01	0.00	0.00	0.00	0.00	0.00	0.00	0.00	0.00	0.01	0.01	0.00	0.00	0.00	0.00	0.85
3391.5	29	0.00	0.00	0.00	0.09	0.00	0.00	0.00	0.00	0.00	0.00	0.01	0.04	0.00	0.00	0.00	0.00	0.00	0.00	0.00	0.00	0.00	0.00
3457.1	30	0.00	0.00	0.00	0.00	0.00	0.00	0.01	0.02	0.01	0.00	0.01	0.00	0.02	0.00	0.01	0.00	0.06	0.05	0.08	0.00	0.00	0.00
3497.9	31	0.00	0.00	0.00	0.00	0.00	0.00	0.00	0.10	0.04	0.00	0.00	0.00	0.01	0.00	0.03	0.01	0.01	0.00	0.04	0.00	0.00	0.00
3730.0	32	0.01	0.00	0.00	0.00	0.00	0.00	0.00	0.09	0.00	0.00	0.00	0.00	0.00	0.00	0.13	0.00	0.00	0.00	0.01	0.00	0.00	0.00
3789.0	33	0.00	0.00	0.01	0.00	0.00	0.00	0.04	0.00	0.00	0.00	0.00	0.00	0.07	0.00	0.00	0.06	0.00	0.00	0.00	0.01	0.00	0.05
3881.0	34	0.00	0.05	0.04	0.00	0.00	0.00	0.01	0.00	0.00	0.00	0.00	0.00	0.01	0.00	0.00	0.04	0.00	0.00	0.00	0.01	0.00	0.00

Figure 9: MAC values between 22 experimentally identified and 34 calculated with FEM modes

the model updating, only the numerical values of those parameters that are identified to be influential will be adjusted until the objective function is minimized.

Limiting the number of parameters to be adjusted is necessary since if a high number of parameters are used in the adjustment, it is possible to obtain good adjustments of the output parameters, having a large number of variables with which to adjust; however, the values obtained will not be reliable and likely would not be too realistic.

	Test		Initial FEM			
Type	Nº	Freq (Hz)	Freq (Hz)	Diff	Diff (%)	MAC
(1 1)	1	154	170.6	16.6	10.8%	0.99
(0 2)	2	207	222.0	15.1	7.3%	1.00
(2 0)	3	273	301.7	28.3	10.4%	0.99
(1 2)	4	382	417.7	35.8	9.4%	0.95
(2 1)	5	401	442.0	40.8	10.2%	0.93
(0 3)	6	622	674.0	52.4	8.4%	0.99
(3 0)	7	717	793.1	76.4	10.7%	0.91
(1 3)	8	753	821.0	67.7	9.0%	0.89
(3 1)	9	864	966.3	101.8	11.8%	0.98
(2 3)	10	1174	1283.5	109.0	9.3%	0.96
(3 2)	11	1215	1332.8	117.9	9.7%	0.84
(1 4)	12	1359	1493.7	134.8	9.9%	0.97
(4 0)	13	1433	1568.6	135.2	9.4%	0.96
(4 1)	14	1545	1696.4	151.7	9.8%	0.96
(3 3)	15	1740	1900.7	160.3	9.2%	0.94
(2 4)	16	1777	1939.0	161.8	9.1%	0.90
(4 2)	17	1928	2123.3	194.8	10.1%	0.93
(0 5)	18	1987	2184.6	197.6	9.9%	0.46
(1 5)	19	2092	2316.9	224.4	10.7%	0.55
(3 4)	20	2405	2630.2	225.2	9.4%	0.74
(4 3)	21	2469	2694.3	225.6	9.1%	0.94
(0 6)	22	2973	3239.4	266.0	8.9%	0.85
			μ =	**124.5**	**9.7%**	**0.89**
			σ =	**76.7**	**0.9%**	**0.14**

Figure 10: Comparative between test and FEM results

One way of performing sensitivity analysis is based on computing derivatives around a baseline point, a so-called local approach. This method can be very effective and is usually cheap but, however, does not paint a complete picture, because it is inherently local. Instead, a global sensitivity analysis, as MCS method, paints a more complete picture as it explores the full space of the input factors [27].

The selected parameters to be used in the sensitivity analysis are the

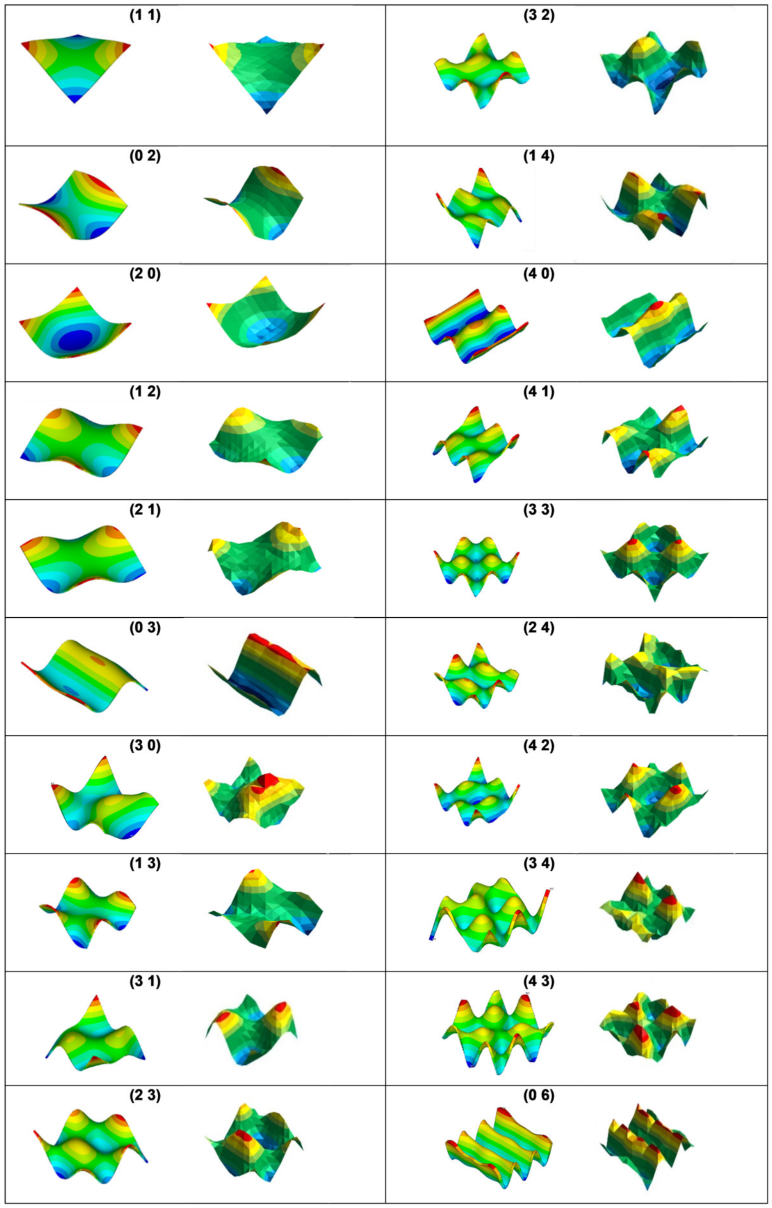

Figure 11: Numerical and experimental modal forms for the first 20 modes with a MAC value close to or greater than 0.8.

mechanical properties shown in Table 4, as well as the density and lamina thickness. The first step is to perform an extensive MCS study, in which a random sample with a sufficiently high number of cases is created, so that the results are statistically significant. A sample of 500 sets of variables has been used, each of which includes a value for the eleven parameters considered.

Both for sensitivity analysis and for model updating, it is assumed the uniformity in all the physical parameters. Thus, the changes of their values are applied to the whole plate uniformly.

The values are generated assuming a normal probability density function for all the variables used, whose mean and standard deviation are shown in Table 4. In addition, upper and lower limits for each parameter are established as the mean values ± 2.5 times the standard deviation. The probability density function of the sample corresponding to the Young modulus E_1 is shown in Fig. 12 as example, where the function corresponding to the sample and analytical normal distribution can be compared.

The set of parameters of each point of the sample is entered as input data in the FEM and the corresponding modal parameters are obtained. The modal pairing with the experimental data is carried out obtaining the values of the numerical frequencies, paired with the 20 first experimental ones, and the value of the corresponding 20 MACs.

The modal pairing with the experimental data is carried out and as output the value of the numerical frequencies paired with the 20 first experimental ones and the value of the corresponding 20 MACs are obtained.

Between the 500 samples that form the input and the 500 outputs, a correlation analysis is performed using the Pearson correlation coefficient,

Parameter	Mean value/deviation	Limits	Units
E_1	139/27.8	69.5/208.5	GPa
E_2	9/1.8	4.5/13.5	GPa
E_3	9/1.8	4.5/13.5	GPa
ν_{12}	0.309/0.062	0.154/0.463	-
ν_{13}	0.309/0.062	0.154/0.463	-
ν_{23}	0.309/0.062	0.154/0.463	-
G_{12}	5/1	2.5/7.5	GPa
G_{13}	5/1	2.5/7.5	GPa
G_{23}	4.5/0.9	2.25/6.75	GPa
Density	1580/316	790/2370	kg/m^3
Lamina thickness	0.191/0.038	0.095/0.286	mm

Table 4: Parameters used in the sensitivity analysis.

which is a measure of the linear relationship between two quantitative random variables. Unlike the covariance, the Pearson correlation ($\rho_{x,y}$) is independent of the scale of measurement of the variables, being the expression that allows to calculate it:

$$\rho_{x,y} = \frac{\sigma_{x,y}}{\sigma_x \sigma_y} \quad (3)$$

Where:

- $\sigma_{x,y}$ is the covariance of (X, Y)
- σ_x is the standard deviation of the variable X
- σ_y is the standard deviation of the variable Y

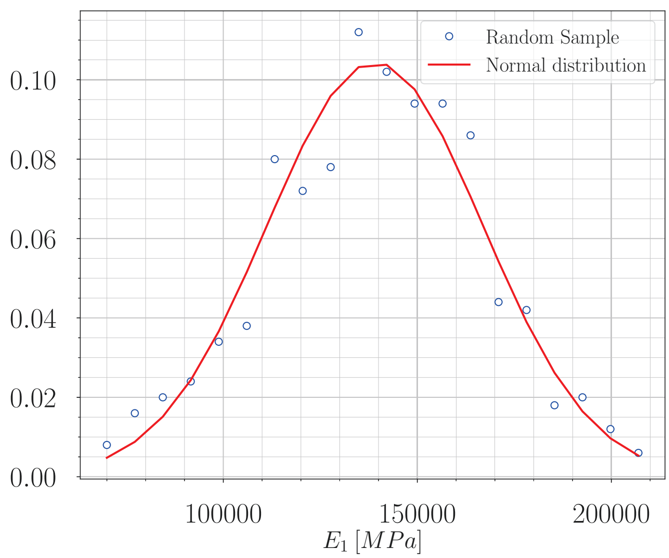

Figure 12: Probability density function for longitudinal modulus E_1.

In a less formal way, the Pearson correlation coefficient can be defined as an index that can be used to measure the degree of relationship of two variables. This approach allows to analyse the degree of influence of each parameter in each of the first 20 estimated frequencies and $MACs$ in relation to the numerical modes. Thus, the final output will be a matrix of as many rows as parameters are analysed and as many columns as outputs will be evaluated.

Pearson coefficients with high absolute value indicate, in general, a high correlation between the parameter and the respective output. In the case that the coefficient is positive, the relationship is direct; that is, increments of the input parameter induce increments in the output parameter. If the value is negative, the relationship is the reverse. Fig. 13 shows the correlation of the frequency of the first vibration mode of the plate with the parameters ply thickness, density and Poisson coefficient in the direction 13, as examples of a high direct correlation, a moderate inverse correlation and an almost zero correlation. That means a high Pearson coefficient in the first case, a medium negative coefficient in the second, and a nearly zero value in the third.

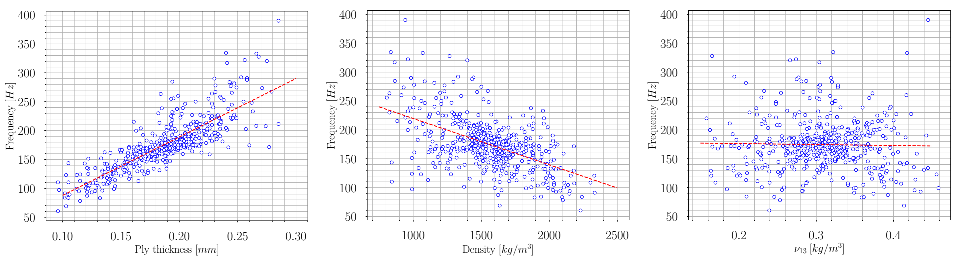

(a) Lamina thickness (b) Density (c) Poisson coefficient 13

Figure 13: Dependence of the first natural frequency

Fig. 14 shows the correlation matrix between all the parameters considered and all the outputs of interest. It is usual practice to consider that the correlation is negligible when the absolute value of the coefficient is less than 0.3, for this reason that range of values is not highlighted. The parameters whose correlations are always (with some exceptions) in that interval will not be used in the adjustment, but will be left with the manufacturer provided values.

It can be seen that ply thickness and, to a lesser extent, the density and the Young modulus E_1, are the parameters that influence the frequency values. On the other hand, the MAC values are influenced by the longitudinal modulus E_1 and E_2, and the shear modulus G_{12} (the influence of the rest of the parameters can be considered negligible, since it is less than 0.3 except in isolated cases). These results should be deeply analysed. To this end

	E_1	E_2	E_3	ν_{12}	ν_{13}	ν_{23}	G_{12}	G_{13}	G_{23}	Density	Thickness
F1	0.39	0.08	0.10	-0.12	-0.02	0.03	-0.02	0.05	-0.01	-0.53	0.83
F2	0.37	0.09	0.09	-0.11	-0.02	0.03	0.00	0.04	-0.01	-0.53	0.84
F3	0.40	0.10	0.09	-0.10	-0.02	0.03	-0.04	0.04	-0.01	-0.53	0.84
F4	0.39	0.09	0.09	-0.11	-0.02	0.03	-0.02	0.05	-0.01	-0.53	0.83
F5	0.39	0.08	0.09	-0.12	-0.02	0.03	-0.02	0.05	-0.01	-0.53	0.83
F6	0.38	0.11	0.09	-0.10	-0.02	0.03	-0.02	0.05	-0.01	-0.53	0.83
F7	0.39	0.09	0.09	-0.11	-0.02	0.03	-0.03	0.05	-0.01	-0.54	0.83
F8	0.38	0.09	0.09	-0.11	-0.02	0.03	-0.01	0.05	-0.01	-0.54	0.83
F9	0.40	0.09	0.09	-0.11	-0.02	0.03	-0.03	0.05	-0.01	-0.53	0.83
F10	0.39	0.09	0.09	-0.11	-0.02	0.03	-0.03	0.05	-0.01	-0.54	0.83
F11	0.39	0.09	0.09	-0.11	-0.02	0.03	-0.03	0.05	-0.01	-0.54	0.83
F12	0.38	0.10	0.09	-0.11	-0.02	0.03	-0.03	0.05	-0.01	-0.54	0.83
F13	0.40	0.09	0.09	-0.11	-0.02	0.03	-0.03	0.05	-0.01	-0.54	0.83
F14	0.40	0.09	0.09	-0.11	-0.02	0.03	-0.03	0.05	-0.01	-0.54	0.83
F15	0.39	0.09	0.09	-0.11	-0.02	0.03	-0.03	0.05	0.00	-0.54	0.83
F16	0.39	0.09	0.09	-0.11	-0.02	0.03	-0.03	0.05	0.00	-0.54	0.83
F17	0.39	0.09	0.09	-0.11	-0.02	0.03	-0.03	0.06	0.00	-0.54	0.82
F18	0.39	0.09	0.09	-0.11	-0.02	0.03	-0.03	0.06	0.00	-0.54	0.82
F19	0.38	0.10	0.09	-0.11	-0.03	0.02	-0.02	0.05	-0.01	-0.54	0.82
F20	0.35	0.09	0.08	-0.10	-0.02	0.02	-0.02	0.03	-0.01	-0.53	0.83

	E_1	E_2	E_3	ν_{12}	ν_{13}	ν_{23}	G_{12}	G_{13}	G_{23}	Density	Thickness
Max/Min	0.40	0.11	0.10	0.12	0.03	0.03	0.04	0.06	0.01	-0.54	0.84

(a) Frequencies

	E_1	E_2	E_3	ν_{12}	ν_{13}	ν_{23}	G_{12}	G_{13}	G_{23}	Density	Thickness
MAC1	-0.14	0.71	-0.06	0.37	-0.03	0.10	-0.34	-0.11	-0.17	-0.12	0.34
MAC2	-0.01	0.67	-0.08	0.27	0.04	0.14	-0.53	-0.03	-0.07	-0.09	0.03
MAC3	0.36	-0.51	0.08	-0.28	0.02	0.01	0.32	0.03	0.07	0.06	0.07
MAC4	0.56	0.23	0.03	0.13	0.05	0.06	-0.75	-0.10	-0.06	-0.12	0.04
MAC5	0.29	0.38	0.03	0.16	0.00	0.09	-0.45	-0.27	0.01	-0.09	0.28
MAC6	-0.64	-0.08	-0.05	-0.09	-0.05	-0.03	0.75	0.02	0.10	0.12	0.03
MAC7	-0.75	0.41	-0.09	0.19	-0.07	0.03	0.44	-0.04	0.00	0.08	0.08
MAC8	0.13	-0.56	0.08	-0.26	-0.04	-0.06	0.44	0.01	0.05	0.14	-0.11
MAC9	-0.26	0.37	-0.11	0.09	0.06	0.13	0.15	0.04	0.08	0.02	0.06
MAC10	0.46	0.26	0.00	0.19	0.07	0.07	-0.77	-0.02	-0.06	-0.11	-0.07
MAC11	-0.76	0.29	-0.06	0.12	-0.06	0.03	0.54	-0.05	0.06	0.09	0.04
MAC12	-0.78	0.25	-0.08	0.08	-0.06	0.01	0.58	-0.02	0.07	0.10	0.04
MAC13	-0.03	0.13	-0.06	-0.01	0.07	0.10	0.15	0.02	0.09	0.03	0.06
MAC14	0.23	-0.40	0.09	-0.14	0.02	0.04	0.33	0.00	0.04	0.08	-0.02
MAC15	-0.70	0.62	-0.11	0.25	-0.04	0.06	0.17	-0.05	-0.01	0.01	0.10
MAC16	-0.63	0.66	-0.10	0.25	-0.04	0.08	0.10	-0.07	-0.02	0.00	0.14
MAC17	0.39	-0.71	0.09	-0.27	0.05	-0.06	0.21	0.11	0.09	0.08	-0.23
MAC18	0.68	-0.07	0.10	0.26	0.00	0.02	-0.40	-0.06	-0.23	-0.13	0.37
MAC19	-0.57	0.41	-0.01	0.14	-0.08	0.06	0.35	-0.14	0.00	0.05	0.18
MAC20	0.16	0.54	-0.03	0.32	0.03	0.10	-0.55	-0.09	-0.10	-0.18	0.30

	E_1	E_2	E_3	ν_{12}	ν_{13}	ν_{23}	G_{12}	G_{13}	G_{23}	Density	Thickness
Max/Min	-0.78	0.71	-0.11	0.37	-0.08	-0.06	-0.77	-0.27	-0.23	-0.18	0.37

(b) MAC

Figure 14: Correlation matrix resulting from sensitivity analysis

in Fig. 15 it can be seen the dependence of MAC value of mode 19 with respect to longitudinal modulus E_1. Despite having a moderate correlation coefficient value (-0.57), because the adjustment to a regression line is good, this adjustment line shows a nearly zero slope. To explain the above, Fig. 16 shows that standard deviations of MAC values are extremely small, which corresponds to very close extreme values found in the sample.

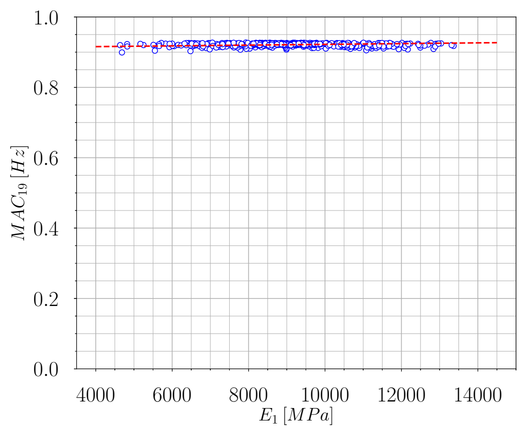

Figure 15: Dependence of MAC value of mode 19 on the longitudinal modulus E_1.

Fig. 17 shows that the covariance of the MAC values with respect to all the adjustment parameters is practically null, which indicates an almost null dependence on them. Therefore, the moderate or even high values of the correlation coefficient that appeared in the correlation matrix for the MAC values were due to the low values of its standard deviations, which are in the denominator of the expression of the correlation coefficient, but they do not indicate a dependency relationship.

Thus, the three parameters that will be used in the model updating process will be those that influence the frequency values: ply thickness, density and longitudinal modulus (E_1). By varying those global parameters, variation of the frequency are expected but not of the mode shapes.

Parámetro	σ	Mín	Máx
MAC1	0.00	0.99	0.99
MAC2	0.00	0.96	0.97
MAC3	0.00	0.98	0.99
MAC4	0.00	0.82	0.83
MAC5	0.00	0.85	0.86
MAC6	0.00	0.97	0.97
MAC7	0.01	0.43	0.50
MAC8	0.01	0.75	0.80
MAC9	0.00	0.96	0.96
MAC10	0.00	0.90	0.91
MAC11	0.00	0.90	0.92
MAC12	0.00	0.91	0.94
MAC13	0.00	0.96	0.96
MAC14	0.00	0.96	0.96
MAC15	0.02	0.81	0.94
MAC16	0.01	0.76	0.81
MAC17	0.00	0.90	0.92
MAC18	0.03	0.49	0.71
MAC19	0.00	0.90	0.93
MAC20	0.00	0.43	0.44

Figure 16: Standard deviation and extreme values of obtained MACs.

4.3. Parameter adjustment

As abovementioned, twenty-two modes have been experimentally identified with relatively high values of the Modal Assurance Criteria, comparing modes shape with those numerically obtained from the FEM model. However, considerable discrepancies between the numerically calculated and the corresponding experimentally measured modal characteristics of the plates have been encountered, as shown in Fig. 10. The objective of the process of adjustment of the model is, starting from its manufacturer provided values in Table 4 to find the values which achieve a better adjustment between the

	E_1	E_2	E_3	ν_{12}	ν_{13}	ν_{23}	G_{12}	G_{13}	G_{23}	Density	Thickness
MAC1	0.000	0.000	0.000	0.000	0.000	0.000	0.000	0.000	0.000	0.000	0.000
MAC2	0.000	0.000	0.000	0.000	0.000	0.000	0.000	0.000	0.000	0.000	0.000
MAC3	0.000	0.000	0.000	0.000	0.000	0.000	0.000	0.000	0.000	0.000	0.000
MAC4	0.000	0.000	0.000	0.000	0.000	0.000	0.000	0.000	0.000	0.000	0.000
MAC5	0.000	0.000	0.000	0.000	0.000	0.000	0.000	0.000	0.000	0.000	0.000
MAC6	0.000	0.000	0.000	0.000	0.000	0.000	0.000	0.000	0.000	0.000	0.000
MAC7	-0.001	0.001	0.000	0.000	0.000	0.000	0.001	0.000	0.000	0.000	0.000
MAC8	0.000	-0.001	0.000	0.000	0.000	0.000	0.000	0.000	0.000	0.000	0.000
MAC9	0.000	0.000	0.000	0.000	0.000	0.000	0.000	0.000	0.000	0.000	0.000
MAC10	0.000	0.000	0.000	0.000	0.000	0.000	0.000	0.000	0.000	0.000	0.000
MAC11	0.000	0.000	0.000	0.000	0.000	0.000	0.000	0.000	0.000	0.000	0.000
MAC12	0.000	0.000	0.000	0.000	0.000	0.000	0.000	0.000	0.000	0.000	0.000
MAC13	0.000	0.000	0.000	0.000	0.000	0.000	0.000	0.000	0.000	0.000	0.000
MAC14	0.000	0.000	0.000	0.000	0.000	0.000	0.000	0.000	0.000	0.000	0.000
MAC15	-0.003	0.002	0.000	0.001	0.000	0.000	0.001	0.000	0.000	0.000	0.000
MAC16	-0.001	0.001	0.000	0.000	0.000	0.000	0.000	0.000	0.000	0.000	0.000
MAC17	0.000	0.000	0.000	0.000	0.000	0.000	0.000	0.000	0.000	0.000	0.000
MAC18	0.003	0.000	0.001	0.001	0.000	0.000	-0.002	0.000	-0.001	-0.001	0.002
MAC19	0.000	0.000	0.000	0.000	0.000	0.000	0.000	0.000	0.000	0.000	0.000
MAC20	0.000	0.000	0.000	0.000	0.000	0.000	0.000	0.000	0.000	0.000	0.000

Figure 17: Covariance matrix resulting from sensitivity analysis.

numerical and the experimental results.

The objective will essentially be to find the minimum of a function, the so-called "objective function", which is an evaluation of the deviation between the numerical model and the experimental results. In this way, when the objective function is zero, it means that both set of results are coincident. There are several strategies to solve this problem. Computational intelligence techniques as neural networks, particle swarm and genetic-algorithm-based methods, simulated annealing or response surface method [28, 29]. Gradient-based methods, as one of the ANSYS own optimization algorithms, would be an alternative. Both types of strategies have been used in previous works [30, 31] of the authors, obtaining similar results. In the present work gradient-based ANSYS optimization algorithm has been chosen.

The main author has used both types of strategies in previous works

[30, 31], obtaining similar results. In the present work gradient-based ANSYS optimization algorithm has been chosen.
The independent variables in the optimization analysis are the design variables, that in the present case are the three parameters to which the model is more sensitive, subjected to a series of restrictions represented by their upper and lower margins of variation. Table 5 contains the definition of these design variables.

Parameter	**Mean value/deviation**	**Limits**	**Units**
E_1	139/27.8	69.5/208.5	GPa
Density	1580/316	790/2370	kg/m^3
Lamina thickness	0.191/0.038	0.095/0.286	mm

Table 5: Parameters to be adjusted.

Although there are various possibilities for defining the objective function, a weighted sum of differences between the experimental modal data (eigenfrequencies and mode shapes) and the corresponding analytical predictions is one of the most common in these kinds of work [31, 32]:

$$f = \sum_{i}^{n} \left[c_i \left| \frac{f_{i,exp} - f_{i,FEM}}{f_{i,exp}} \right| + d_i \left(1 - MAC_i\right) \right] \tag{4}$$

Where:

- n is the number of modes used in the adjustment
- $f_{i,exp}$ and $f_{i,FEM}$ are, respectively, the frequency of the i-th mode identified in the tests and calculated with the numerical model and paired with the previous one through the MAC value

- c_i and d_i are the weighting factors that are used to give more importance to the frequencies characterized with greater precision, if that is the case, and to the criterion depending on the modal forms

- MAC_i is the highest value of the MAC obtained for the i-th mode identified in the tests when compared with the n numerical modes; that is, $MAC_i = max(MAC_{ij})$.

In the present case, as it has been seen in the previous section, the MAC values are not sensitive to the parameters of the model. Therefore they are not included in the calculation of the objective function, being all the coefficients (d_i) zero. On the other hand, the MAC value can be considered as an indicator of the precision with which the experimental modes have been identified. That is, it is considered a priori that the modes with the lowest MAC have been identified with less precision than those with the high MAC. For this reason, it has been considered appropriate to use the MAC value as a factor for weighting (c_i) the frequency differences.

Therefore, the final expression of the objective function will be:

$$f = \sum_{i}^{n} \left[MAC_i \left| \frac{f_{i,exp} - f_{i,FEM}}{f_{i,exp}} \right| \right] \tag{5}$$

The optimization can be performed using one of the available optimization methods in ANSYS:

- Subproblem approximation method

- First order optimization method

The first is a zero-order method (it requires only the values of the dependent variables but not their derivatives) which establishes the relationship between the objective function and the design variables by curve fitting. It is a general method that can be applied efficiently to a wide range of engineering problems.

The second, unlike the first, uses derivative information and minimizes the real objective function, not an approximation. It is a highly accurate method that can be computationally more intense than the first one. Therefore, in this case adjustments have been made by both methods. A first adjustment is made with the Subproblem approximation method. Subsequently, a new adjustment is made with the First Order optimization method but taking as starting design the best result of the previous adjustment. This improves computational efficiency to reach the best solution.

Table 6 shows the values obtained for the three parameters after the adjustment process.

Parameter	**Initial value**	**Adjusted value**	**Units**
E_1	139	135	GPa
Density	1580	1623	kg/m^3
Lamina thickness	0.191	0.178	mm

Table 6: Adjusted values of the parameters

As can be seen, the percentage variation of the value of the parameters is not important (between 3% and 7%). However, its effect is important, as shown in Fig. 18, where can be seen that the total error drops from an average of 125 Hz to only 6 Hz, which represents a decrease in relative terms from an average of 10% to only 0.6%. On the other hand, MAC values have not been improved, which can be explained by the limits of accuracy of the experimental method. Experimental mode shapes are not smooth enough to obtain higher MAC values.

	Test		Initial FEM				Updated FEM			
Type	Nº	Freq (Hz)	Freq (Hz)	Diff	Diff (%)	MAC	Frec (Hz)	Diff	Diff (%)	MAC
(1 1)	1	154	170.6	16.6	10.8%	0.99	155.4	1.5	0.9%	0.99
(0 2)	2	207	222.0	15.1	7.3%	1.00	202.4	-4.5	-2.2%	1.00
(2 0)	3	273	301.7	28.3	10.4%	0.99	274.6	1.3	0.5%	0.99
(1 2)	4	382	417.7	35.8	9.4%	0.95	380.9	-1.0	-0.3%	0.95
(2 1)	5	401	442.0	40.8	10.2%	0.93	403.0	1.8	0.5%	0.93
(0 3)	6	622	674.0	52.4	8.4%	0.99	614.6	-6.9	-1.1%	0.99
(3 0)	7	717	793.1	76.4	10.7%	0.91	723.1	6.3	0.9%	0.90
(1 3)	8	753	821.0	67.7	9.0%	0.89	749.4	-3.9	-0.5%	0.89
(3 1)	9	864	966.3	101.8	11.8%	0.98	881.2	16.7	1.9%	0.98
(2 3)	10	1174	1283.5	109.0	9.3%	0.96	1172.0	-2.5	-0.2%	0.96
(3 2)	11	1215	1332.8	117.9	9.7%	0.84	1216.9	2.1	0.2%	0.84
(1 4)	12	1359	1493.7	134.8	9.9%	0.97	1364.0	5.1	0.4%	0.98
(4 0)	13	1433	1568.6	135.2	9.4%	0.96	1431.4	-2.0	-0.1%	0.96
(4 1)	14	1545	1696.4	151.7	9.8%	0.96	1548.8	4.2	0.3%	0.96
(3 3)	15	1740	1900.7	160.3	9.2%	0.94	1736.9	-3.5	-0.2%	0.94
(2 4)	16	1777	1939.0	161.8	9.1%	0.90	1772.1	-5.1	-0.3%	0.90
(4 2)	17	1928	2123.3	194.8	10.1%	0.93	1940.1	11.6	0.6%	0.93
(0 5)	18	1987	2184.6	197.6	9.9%	0.46	1996.2	9.2	0.5%	0.46
(1 5)	19	2092	2316.9	224.4	10.7%	0.55	2118.1	25.7	1.2%	0.55
(3 4)	20	2405	2630.2	225.2	9.4%	0.74	2405.1	0.1	0.0%	0.74
(4 3)	21	2469	2694.3	225.6	9.1%	0.94	2464.4	-4.3	-0.2%	0.94
(0 6)	22	2973	3239.4	266.0	8.9%	0.85	2963.7	-9.7	-0.3%	0.85
			μ =	**124.5**	**9.7%**	**0.89**		**5.9**	**0.6%**	**0.89**
			σ =	**76.7**	**0.9%**	**0.14**		**8.2**	**0.8%**	**0.14**

Figure 18: Comparison between model and tests before and after the adjustment process

Finally, the natural frequencies are calculated in the calibrated model of the plate, eliminating the mass of the accelerometer. The results are shown in Table 7.

5. Experimental validation of updated properties

In order to obtain a validation of model updating, the value of the total weight of the plates, their thickness and stiffness have been verified experi-

Nº	Type	f (Hz)	Nº	Type	f (Hz)	Nº	Type	f (Hz)
1	(1 1)	158	11	(2 3)	1174	21	(1 5)	2115
2	(0 2)	202	12	(0 4)	1198	22	(5 0)	2336
3	(2 0)	278	13	(3 2)	1218	23	(3 4)	2402
4	(1 2)	385	14	(1 4)	1366	24	(4 3)	2462
5	(2 1)	407	15	(4 0)	1430	25	(5 1)	2475
6	(0 3)	617	16	(4 1)	1549	26	(2 5)	2574
7	(3 0)	728	17	(3 3)	1737	27	(5 2)	2828
8	(2 2)	732	18	(2 4)	1771	28	(0 6)	2964
9	(1 3)	750	19	(4 2)	1940	29	(1 6)	3107
10	(3 1)	888	20	(0 5)	1993	30	(3 5)	3161

Table 7: Frequencies obtained from updated model without accelerometer mass

mentally.

The theoretical weight of the plates would be 569 g (assuming an exact constant thickness of 4 mm and the theoretical density of 1580 kg/m^3). The actual weight of the plates has been verified with a high precision balance, obtaining a value of 552 g, which represents a weight reduction of almost 3%.

The thickness has also been measured, by ultrasonic inspection in a very fine mesh of 250x250 points. The result of this inspection is shown in Fig. 19, where it is observed that the thickness, although showing slight variations, is quite uniform around 3.7 mm. This value is very well adjusted to that of the optimized ply thickness parameter, which would give a thickness of 0.178 mm x 21 plies = 3.74 mm.

On the other hand, if the optimized thickness value together with the

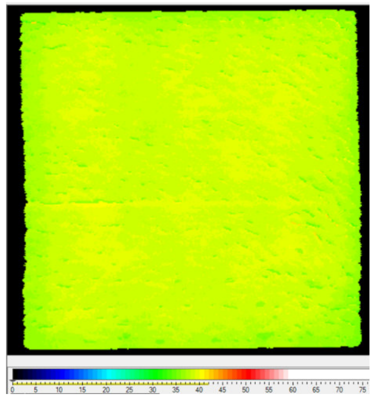

Figure 19: Thickness measured by ultrasonic inspection.

density value of 1623 kg/m^3 is considered, an optimized weight of 546 g. would be obtained, which also adjusts to the measured value (552 g).

	Measured	**Preliminar**	**Diff.**	**Updated**	**Diff.**
Thickness (mm)	3.72	4.0	7.5%	3.74	0.6%
Density (kg/m^3)	1650	1580	-4.2%	1623	-1.6%
Weight (g)	552	569	3.0%	546	-1.1%
Stiffness (kN/mm)*	0.304	0.362	19.4%	0.286	-5.8%

* Mean value of the results obtained from the QSL tests

Table 8: Comparison of measured, preliminar and updated values of the parameters.

Additionally, to have an experimental measurement that is also influenced by elastic properties, Quasi Static Loading (QSL) tests were performed to measure the transverse stiffness of the plates. The support and the indentator were changed from the standard test method for QSL, ASTM-D6264, in order to adapt it to specimens size (300 x 300 *mm*) and shape. Accordingly, the support type was rectangular instead of circular support, to simply support

10 *mm* along the outer border of the specimen as can be observed in Fig.20 . The indentator was a 40 mm steel ball (57-66 HRC) subjected to a constant displacement velocity of 1.25 mm/min perpendicular to the plate, imposed by an Universal testing machine (Instron 8516). Loading force and plate central deflection data were recorded at a sampling rate of 100 Hz.

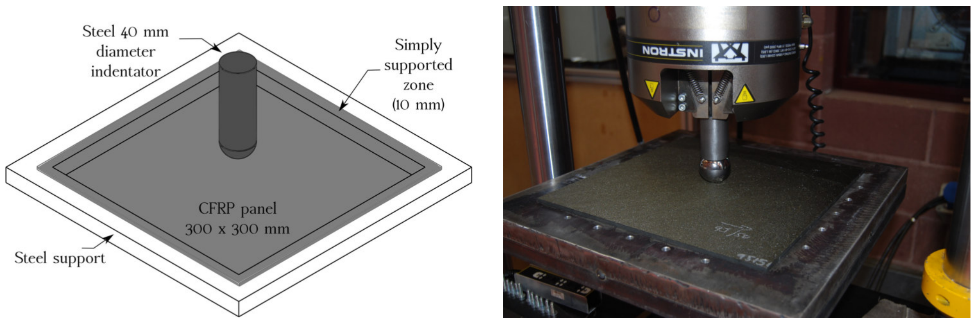

(a) (b)

Figure 20: Scheme and picture of QSI tests

The summary of results is shown in Table 8 and Fig. 21 . As can be seen, the optimized values are much more adjusted to the measured values than the initial ones.

6. Benchmarking tests

Tests have been performed on the benchmarking set of 32 plies composite plate specimens. To obtain the modal characteristics of the six plates, a modal testing was performed using the abovementioned methodology. The values of the 19 identified frequencies are shown in Fig. 22. As can be seen, all the modes have been identified in the four plates again with very stable values of the frequency.

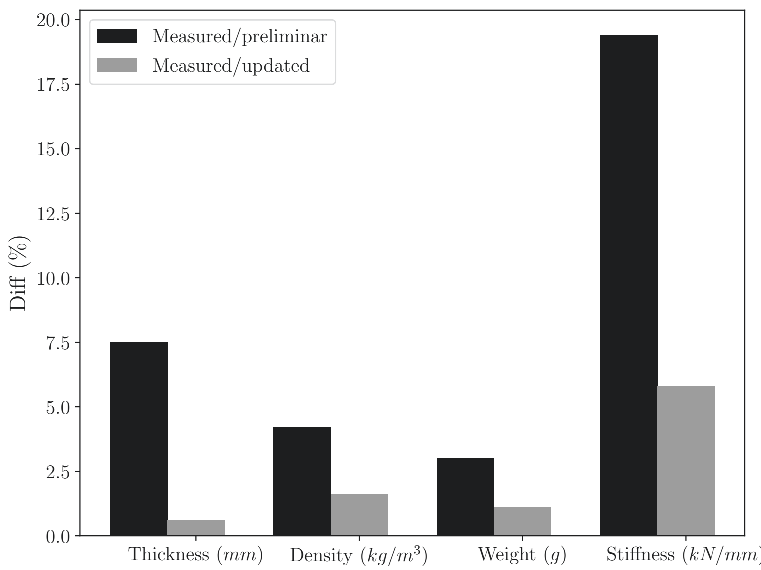

Figure 21: Comparison of differences between measured and preliminar, and measured and updated values of the parameters .

In parallel, a new FEM model of the plates has been constructed, based on the preliminar characteristics of the plates. The first 34 natural frequencies obtained from the model are represented in Table 9.

In Fig. 22, MAC values corresponding to the comparison between the 19 experimental modes and the first 34 modes calculated with the numerical model are also shown. It can be pointed out that in the case of three of the plates (0, I and III) those MAC values are almost always higher than 0.8, whereas in the case of plates II, IV and V lower values are obtained. For this reason, the data have been processed as corresponding to three different setups of the same test, identifying average values of frequencies and mode shapes, but using only the results corresponding to plates 0, I and III.

	Frequencies (Hz)												MAC					
Type	Initial FEM (f_3)			0	I	II	III	IV	V	μ	σ	Diff	0	I	II	III	IV	V
(1 1)	1	242.7	1	224	224	225	226	226	225	225	0.4%	8%	0.99	1.00	0.99	1.00	1.00	1.00
(0 2)	2	342.0	2	317	318	322	321	323	322	321	0.6%	7%	0.99	0.99	0.52	0.99	1.00	0.99
(2 0)	3	456.3	3	422	423	423	426	427	426	424	0.4%	8%	0.99	0.99	0.53	0.99	0.99	0.99
(1 2)	4	605.1	4	558	559	561	564	565	563	562	0.5%	8%	0.99	0.99	0.98	0.99	0.98	1.00
(2 1)	5	649.0	5	599	600	599	605	605	604	602	0.4%	8%	1.00	1.00	0.99	1.00	0.68	1.00
(0 3)	6	1008.3	6	932	932	938	942	946	944	939	0.6%	7%	0.99	0.99	0.97	0.99	0.97	0.99
(2 2)	7	1145.7	7	1059	1059	1063	1067	1069	1068	1064	0.4%	8%	0.99	0.99	0.91	0.99	0.96	0.99
(1 3)	8	1212.0	8	1127	1133	1123	1140	1136	1138	1133	0.5%	7%	0.92	0.92	0.78	0.75	0.88	0.80
(3 1)	10	1432.3	9	1326	1331	1313	1338	1318	1337	1327	0.7%	8%	0.99	0.99	0.63	0.99	0.91	0.99
(2 3)	11	1846.2	10	1718	1710	1720	1731	1715	1720	1719	0.4%	7%	0.98	0.98	0.80	0.98	0.86	0.97
(3 2)	12	1937.2	11	1799	1798	1785	1814	1815	1812	1804	0.6%	7%	0.94	0.89	0.94	0.92	0.83	0.94
(1 4)	14	2190.8	12	2046	2034	2056	2064	2010	2063	2045	0.9%	7%	0.96	0.96	0.92	0.95	0.89	0.93
(4 0)	15	2372.1	13	2209	2209	2227	2223	2242	2230	2223	0.5%	7%	0.88	0.94	0.71	0.90	0.70	0.89
(4 1)	16	2536.7	14	2363	2362	2364	2379	2407	2384	2376	0.7%	7%	0.95	0.96	0.45	0.92	0.18	0.87
(3 3)	17	2723.0	15	2529	2526	2528	2546	2549	2533	2535	0.4%	7%	0.95	0.92	0.59	0.92	0.13	0.89
(2 4)	18	2795.7	16	2594	2600	2606	2621	2629	2611	2610	0.5%	7%	0.90	0.91	0.76	0.89	0.11	0.80
(4 2)	19	3092.9	17	2875	2874	2884	2893	2898	2886	2885	0.3%	7%	0.85	0.83	0.45	0.82	0.35	0.61
(3 4)	22	3707.6	18	3441	3437	3442	3471	3462	3449	3450	0.4%	7%	0.74	0.73	0.26	0.73	0.29	0.60
(4 3)	23	3858.3	19	3580	3579	3585	3617	3612	3601	3596	0.4%	7%	0.64	0.62	0.48	0.71	0.47	0.35
										μ =	**0.5%**	**7.2%**	**0.93**	**0.93**	**0.72**	**0.92**	**0.69**	**0.87**

Figure 22: Comparison between model and tests before and after the adjustment process (benchmarking tests)

Fig. 23 shows these average values together with the differences in frequencies between the paired modes (experimental an numerical) and MAC values. These differences are around 7% in all modes, and MAC values are higher than 0.8 with the exception of mode 8, for which it is 0.65.

In this case, the sensitivity analysis is not performed, as one of the objective of the benchmarking tests is to prove that the previously chosen parameters are able to be used again to obtain a good model updating. Thus, the three parameters that will be used in the process will be again the ply thickness, the density and the longitudinal modulus E_1.

Table 10 shows the values obtained for the three parameters after the adjustment process. As can be seen, the percentage variation of the value of the parameters is low (between 2.8% and 6.1%). However, its effect is important as shown in Fig. 23, where can be seen that the total error drops

Nº	Type	f (Hz)	Nº	Type	f (Hz)	Nº	Type	f (Hz)
1	(1 1)	243	13	(0 4)	1959	25	(5 1)	4020
2	(0 2)	342	14	(1 4)	2191	26	(2 5)	4047
3	(2 0)	456	15	(4 0)	2372	27	(5 2)	4513
4	(1 2)	605	16	(4 1)	2537	28	(0 6)	4723
5	(2 1)	649	17	(3 3)	2723	29	(4 4)	4906
6	(0 3)	1008	18	(2 4)	2796	30	(1 6)	4917
7	(2 2)	1146	19	(4 2)	3093	31	(3 5)	4953
8	(1 3)	1212	20	(0 5)	3222	32	(5 3)	5331
9	(3 0)	1219	21	(1 5)	3397	33	(2 6)	5478
10	(3 1)	1432	22	(3 4)	3708	34	(6 0)	5659
11	(2 3)	1846	23	(4 3)	3858			
12	(3 2)	1937	24	(5 0)	3873			

Table 9: 34 first natural frequencies predicted by FEM for the plates used for benchmarking tests

from an average of 124 Hz to only 3.5 Hz, which represents a decrease in relative terms from an average of 7% to only 0.2%, with a maximum of 0.5%. It can be pointed out that the differences between the model and the experimental results are even lower than the differences between the six plates.

Once again, in order to obtain a validation of model updating, the values of the total weight of the plates, their thickness and stiffness have been verified experimentally. The theoretical weight of the plates would be 853 g (assuming an exact constant thickness of 6 mm and the theoretical density of 1580 kg/m^3). The actual weight of the plates has been verified with

Parameter	Initial value	Adjusted value	Diff(%)	Units
E_1	139	143	2.8	GPa
Density	1580	1644	4.5	kg/m^3
Lamina thickness	0.1875	0.176	6.1	mm

Table 10: Adjusted values of the parameters (benchmarking tests)

	Test		Initial FEM (f_3)				Updated FEM			
Type	Nº	Freq (Hz)	Freq (Hz)	Diff	Diff (%)	MAC	Freq (Hz)	Diff	Diff (%)	MAC
(1 1)	1	225	242.7	-17.9	7.4%	1.00	225.4	-0.6	0.3%	1.00
(0 2)	2	319	342.0	-23.0	6.7%	0.99	317.5	1.5	-0.5%	0.99
(2 0)	3	423	456.3	-33.0	7.2%	1.00	423.9	-0.6	0.1%	1.00
(1 2)	4	561	605.1	-44.5	7.4%	0.99	562.3	-1.8	0.3%	0.99
(2 1)	5	602	649.0	-47.5	7.3%	1.00	603.4	-1.8	0.3%	1.00
(0 3)	6	936	1008.3	-72.7	7.2%	0.99	937.0	-1.5	0.2%	0.99
(2 2)	7	1062	1145.7	-84.2	7.3%	0.99	1066.0	-4.5	0.4%	0.99
(3 0)	8	1134	1218.7	-85.0	7.0%	0.65	1134.1	-0.4	0.0%	0.65
(3 1)	9	1332	1432.3	-100.5	7.0%	1.00	1333.1	-1.4	0.1%	1.00
(2 3)	10	1720	1846.2	-126.6	6.9%	0.99	1719.7	-0.1	0.0%	0.99
(3 2)	11	1804	1937.2	-133.5	6.9%	0.94	1804.9	-1.3	0.1%	0.94
(1 4)	12	2048	2190.8	-143.1	6.5%	0.98	2040.3	7.4	-0.4%	0.98
(4 0)	13	2214	2372.1	-158.6	6.7%	0.94	2211.2	2.3	-0.1%	0.94
(4 1)	14	2368	2536.7	-168.7	6.7%	0.97	2365.5	2.5	-0.1%	0.97
(3 3)	15	2534	2723.0	-189.4	7.0%	0.97	2539.8	-6.2	0.2%	0.97
(2 4)	16	2605	2795.7	-190.8	6.8%	0.95	2607.1	-2.2	0.1%	0.95
(4 2)	17	2881	3092.9	-212.2	6.9%	0.91	2886.5	-5.8	0.2%	0.91
(3 4)	18	3450	3707.6	-257.7	7.0%	0.86	3462.3	-12.5	0.4%	0.86
(4 3)	19	3592	3858.3	-266.1	6.9%	0.80	3604.3	-12.1	0.3%	0.81
			μ =	**124.0**	**7.0%**	**0.94**		**3.5**	**0.2%**	**0.94**
			σ =	**76.9**	**0.3%**	**0.09**		**4.7**	**0.2%**	**0.09**

Figure 23: Comparison between model and tests before and after the adjustment process (benchmarking tests).

a high precision balance, having obtained an average value of 836 g, which represents a weight reduction of a 2%.

On the other hand, the thickness has also been measured, by ultrasonic inspection in a very fine mesh of 250x250 points. The result of this inspection for plate 0, I and III is shown in Fig. 24, where it is observed that the thickness, although showing slight variations, is quite uniform around 5.7 mm. It can be seen that this value is very well adjusted to that of the optimized ply thickness parameter, which would give a thickness of 0.176 mm x 32 plies = 5.62 mm.

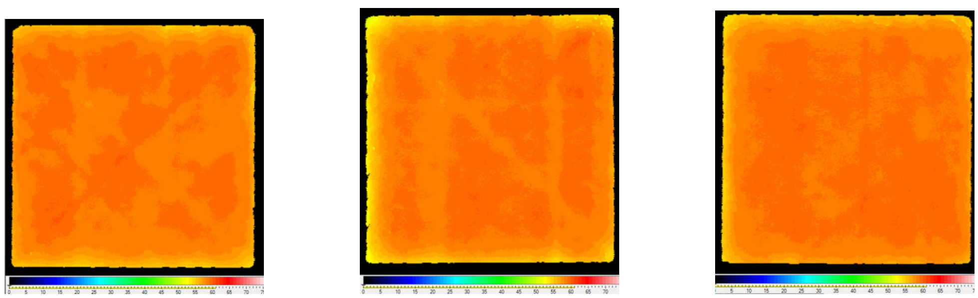

(a) (b) (c)

Figure 24: Thickness measured by ultrasonic inspection for plates 0, I and III (benchmarking tests)

If the optimized thickness value together with the density value of 1644 kg/m^3 are considered, an optimized weight of 832 g would be obtained, which also adjusts to the measured value. And finally, also quasi-static loading (QSL) tests were performed to measure the transverse stiffness of the plates. Measured values of the plates are compared with the values obtained numerically by simulating the QSL tests with the FEM model, considering both, initial and updated values of the parameter. The summary of results is shown in Table 11 and Fig. 25. As can be seen, the optimized values are much more adjusted to the measured values than the initial ones.

On the other hand, it can be pointed out that ultrasonic inspection of

	Measured	**Preliminar**	**Diff.**	**Updated**	**Diff.**
Thickness (mm)	5.72	6.0	4.9%	5.62	-1.7%
Density (kg/m^3)	1624	1580	-2.7%	1623	-0.1%
Weight (g)	836	853	2.1%	832	-0.5%
Stiffness (kN/mm)	0.915*	1.152	25.9%	0.977	6.7%

* Mean value of the results obtained from the QSL tests

Table 11: Comparison of measured, preliminar and updated values of the parameters (benchmarking tests).

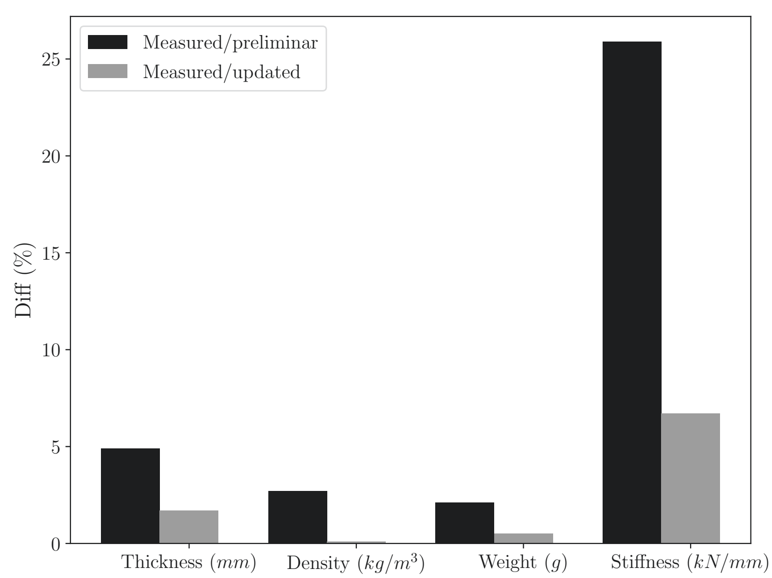

Figure 25: Comparison of differences between measured and preliminar, and measured and updated values of the parameters (benchmarking tests).

plates II, IV and V has demonstrated that there are some minor manufacturing defects in the plates, with zones in which the thickness is higher, as can be seen in Fig. 26. This effect is due to small overlaps that could be produced during the hand lay-up. This could explain the lower MAC values encountered for these plates (Fig. 22) in the comparison with the mode shape obtained from the FEM model, and could be used in future works as a mean to detect manufacturing defects.

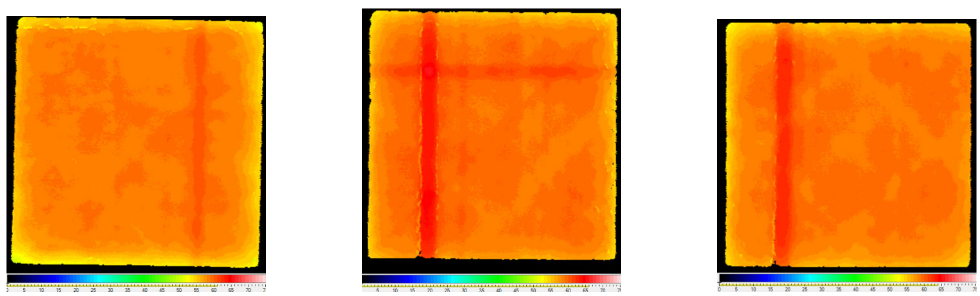

(a) (b) (c)

Figure 26: Thickness measured by ultrasonic inspection for plates II, IV and V(benchmarking tests)

7. Conclusions

In the present work, the methodology for the estimation of some of the material properties of two set of rectangular carbon/epoxy composite plates, using vibration-based experimental data and FEM model updating techniques, has been laid out. The methodology uses the deviation between the experimental modal information (eigenfrequencies and mode shapes) and finite element model to be applied to an optimization process.

A very accurate experimental modal analysis of the plates has been performed, by which up to 22 eigenfrequencies and corresponding mode shapes have been estimated.

By this estimation it has been stated that the numerical model of the plates deviates from their real behaviour, with differences in frequencies between the numerical and experimental modes that are around 10% in all modes.

The sensitivity analysis of the modal characteristics of the plates and material properties, using MCS, showed that the three material parameters with a higher influence are the Young modulus E_1, the density and the lamina thickness, and they are selected for model updating process.

After the model updating it was seen that a low percentage of variation of the values of the parameters adjusted (between 3% and 7%) has an important effect in the total error in frequencies, that drops to only a 0.6%.

The consistency of the adjusted parameter has been experimentally verified by measuring the real weight of the plates, their thickness and stiffness.

The efficiency of the methodology has been proved through benchmarking tests. The same process has been used in a second set of composite plates with a different thickness and stacking sequence, obtaining again an accurate and physically-sound updated model.

As a result of the whole process, a physically more correct model is obtained on which discrepancies with the corresponding experimentally measured modal parameters are drastically reduced. This model establishes the baseline (pristine situation) of the dynamic behaviour of the set of composite plates. Therefore it could be applied for condition assessment or quality manufacturing control of existing structures through a non-destructive Structural Health Monitoring, and hence it could help to detect degradation or defects of the composite components.

Acknowledgements

This research was done with the financial support of the Spanish Ministry of Economy and Competitiveness under Project reference DPI2013-41094-R, and the Vicerrectorado de Política Científica UC3M (Projects 2014/00006/002 and 2013/00413/003).

References

References

[1] M. A. Pérez, L. Gil, S. Oller, Impact damage identification in composite laminates using vibration testing, Compos. Struct. 108 (2014) 267–276.

[2] W. Fan, P. Qiao, Vibration-based damage identification methods: A review and comparative study, Struct. Hlth. Monit. 10 (1) (2011) 83–111.

[3] S. W. Doebling, C. R. Farrar, M. B. Prime, A summary review of vibration-based damage identification methods, The Shock and Vibration Digest 30 (1998) 91–105.

[4] E. Reynders, System identification methods for (operational) modal analysis: Review and comparison, Arch. Comput. Methods E. 19 (1) (2012) 51–124.

[5] B. Peeters, System identification and damage detection in civil engineering, Ph.D. thesis, Department of Civil Engineering, K.U.Leuven, 2003.

[6] J. Maeck, Damage assessment of civil engineering structures by vibration monitoring, Ph.D. thesis, Department of Civil Engineering, K.U.Leuven, 2003.

[7] C. Surace, R. Saxena, M. Gherlone, H. Darwich, Damage localisation in plate like-structures using the two-dimensional polynomial annihilation edge detection method, J. Sound Vib. 333 (21) (2014) 5412–5426.

[8] Z. Zhang, K. Shankar, T. Ray, E. V. Morozov, M. Tahtali, Vibration-based inverse algorithms for detection of delamination in composites, Compos. Struct. 102 (2013) 226–236.

[9] Z. Zhang, M. He, A. Liu, H. K. Singh, K. R. Ramakrishnan, D. Hui, K. Shankar, E. V. Morozov, Vibration-based assessment of delaminations in FRP composite plates, Compos. Part B-Eng 144 (2018) 254–266.

[10] Y. Yan, L. Yam, Detection of delamination damage in composite plates using energy spectrum of structural dynamic responses decomposed by wavelet analysis, Comput. Struct. 82 (4) (2004) 347–358.

[11] Z. Wei, L. Yam, L. Cheng, Detection of internal delamination in multi-layer composites using wavelet packets combined with modal parameter analysis, Compos. Struct. 64 (3) (2004) 377–387.

[12] L. Yam, Y. Yan, J. Jiang, Vibration-based damage detection for composite structures using wavelet transform and neural network identification, Compos. Struct. 60 (4) (2003) 403–412.

[13] M. Chandrashekhar, R. Ganguli, Damage assessment of composite plate structures with material and measurement uncertainty, Mech. Syst. Signal Pr. 75 (2016) 75–93.

[14] A. Teughels, J. Maeck, D. De Roeck, A finite element model updating method using experimental modal parameters applied on a railway bridge, Proceedings of 7th International Conference on Computer Aided Optimum Design of Structures, Bologna, 2001.

[15] A. Esfandiari, F. Bakhtiari-Nejad, M. Sanayei, A. Rahai, Structural finite element model updating using transfer function data, Comput. Struct. 88 (1) (2010) 54–64.

[16] W. Visser, Updating structural dynamics models using frequency response data, Ph.D. thesis, Department of Mechanical Engineering, Imperial College of Science, Technology and Medicine, London SW7 (1992).

[17] Z.X. Yuan, K.P. Yu, Finite element model updating of damped structures using vibration test data under base excitation, J. Sound Vib. 340 (2015) 303–316.

[18] A. K. Mishra, S. Chakraborty, Development of a finite element model updating technique for estimation of constituent level elastic parameters of FRP plates, Appl. Math. Comput. 258 (2015) 84–94.

[19] A. K. Mishra, S. Chakraborty, Inverse detection of constituent level elastic parameters of FRP composite panels with elastic boundaries using finite element model updating, Ocean Eng. 111 (2016) 358–368.

[20] K. Sepahvand, S. Marburg, Identification of composite uncertain material parameters from experimental modal data, Probabilistic Eng. Mech. 37 (2014) 148–153.

[21] G. Petrone, V. Meruane, Mechanical properties updating of a non-uniform natural fibre composite panel by means of a parallel genetic algorithm, Compos. Part A: Appl. S. 94 (2017) 226–233.

[22] F. Adel, S. Shokrollahi, M. Jamal-Omidi, H. Ahmadian, A model updating method for hybrid composite/aluminum bolted joints using modal test data, J. Sound Vib. 396 (2017) 172–185.

[23] Ansys, User's manual, ANSYS Release 18.1 (2017).

[24] E. Reynders, M. Schevenels, G. Roeck, Macec 3.3: a matlab toolbox for experimental and operational modal analysis, User manual - Report BWM-2014-06, 2014.

[25] IMC Gmbh., Imc famos, Users Manual Version 7.2. Doc. Rev 1, 14.04.2017.

[26] R. Allemagne, The Modal Assurance Criterion (MAC)-twenty years of use and abuse. Sounds and Vibration (2003) 14–21.

[27] M.M.J. Opgenoord , D.L. Allaire, K.E. Willcox, Variance-based sensitivity analysis to support simulation-based design under uncertainty, J. Mech. Design 138 (2016) 111410.

[28] T. Marwala, Finite Element Model Updating Using Computational Intelligence Techniques, Springer Verlag, London, 2010.

[29] M. Friswell, J.E. Mottershead, Finite element model updating in structural dynamics, Springer Science & Business Media 38 (2013).

[30] M. Cuadrado, E. Moliner. Modeling and long term structural health monitoring of Villanueva del Jalón viaduct, Eurodyn 2014, IX International Conference on Structural Dynamics, Porto, 2014.

[31] E. Moliner, M. Cuadrado, Assessment of Long-Term Structural Health at Villanueva del Jalón Viaduct, Proceedings of the Second International Conference on Railway Technology: Research, Development and Maintenance, Civil-Comp Proceedings, 2014.

[32] D. Ribeiro, R. Calçada, R. Delgado, M. Brehm, V. Zabel, Finite element model updating of a bowstring-arch railway bridge based on experimental modal parameters, Eng. Struct. 40 (2012) 413–435.